Design and Analysis of Composite Foundation for High-rise Buildings

K. Watanabe[1], N. Suzuki[2] and M. Sahara[3]
[1,2,3]Geotechnical Engineering Department, Technical Research Institute, Obayashi Corp., Tokyo, Japan
E-mail: watanabe.kazuhiro@obayashi.co.jp

ABSTRACT: A composite foundation combines several types of foundation to support a single superstructure. Thus, this type of foundation should be carefully designed considering the stress in the boundary section caused by the difference in the deformation behaviors of each foundation type. This paper shows two design cases of composite foundations for high-rise buildings. These two foundations were designed by considering the effect of deformation on the results of a static FEM analysis. The slab settlement was measured upon completion of construction. It was confirmed that composite foundations deform within a presupposed range.

KEYWORDS: Composite Foundation, Performance-based Design, FEM

1. INTRODUCTION

A composite foundation combines several types of foundation to support a single superstructure. In Japan, the previous conventional design procedure required a simple pile or spread foundation, and did not permit the use of a composite foundation. The law, which was revised in 2000, now allows the use of a composite foundation subject to confirmation of safety via a performance-based design.

The main problem in composite foundation design is the difference in the deformation behaviors of the pile and spread foundations.

The vertical loads via the pile foundation are considered to constitute a point load on the stress distribution in the ground. Meanwhile, the loads via the spread foundation are treated as a uniformly distributed load. Thus, the ground stress distribution will be biased and complex if different foundation types are used together.

The pile foundations for the lateral loads primary obtain their resistance force from the soil strain. Meanwhile, the spread foundations primary obtain their resistance force from the friction between the foundation and soil. The resistance force caused by friction acts prior to that caused by strain. Thus, a spread foundation is considered to be more rigid than a pile foundation, except in the case of spread foundation slips (Architectural Institute of Japan, 2001).

A composite foundation involves a combination of these different deformation behaviors. Moreover, consideration of the unequal settlement and torsion is important in a performance-based design of a composite foundation (Sahara, 2015).

This paper introduces two practical examples for buildings with composite foundation (labeled A and B). These two foundations are designed by referring to analytical results obtained using the finite element method (FEM), not only to predict the behavior, but also to reflect the influence of the design. The actual slab displacements are measured in both cases. This paper also presents a comparison between the predictive FEM analysis results and measurements.

2. DESIGN PROCEDURE

Figure 1 shows the design procedure for the adopted composite foundations. The procedure begins at the grid model stage. The structural grid model was determined on the condition that the foundations were fixed. The reaction forces were used as input loads in the FEM in the next stage. The specifications of the pile, footing beam, and slab sections were provisionally determined by referring to the calculated stress of the grid model. The FEM model of the composite foundation was built in the subsequent stage, to determine the stiffness of the soil springs. Further, the input loads and the cross-sections of the components provisionally determined in the preceding stage were included in the FEM model. The soil springs determined from the FEM analysis were reflected in the grid model in the next whole-building grid model stage. The acceptability of the sectional forces of each component was examined. The cross-sections of the components were revised and the FEM stage was implemented again if the forces were not acceptable. The rest of the procedure was performed in a straightforward manner after all the cross-sections of the components were determined.

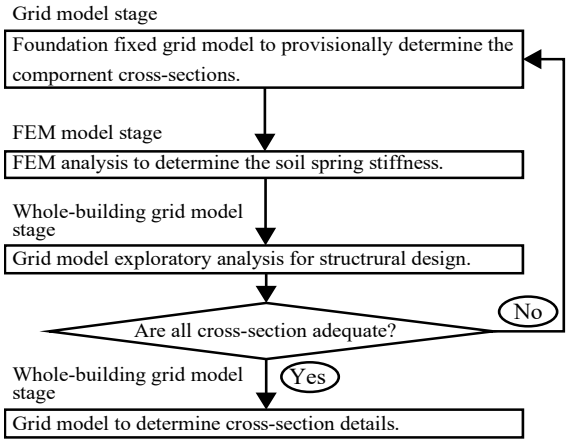

Figure 1 Design procedure

The whole-building grid model comprises only the foundation beam and the superstructure. Thus, the reaction force from the pile was evaluated at the pile head. The sectional forces of each pile body were evaluated separately via *the t-z* analysis and the response deformation method (Coyle and Reese, 1966; Kraft et al., 1981).

This paper primarily describes the FEM stage of the procedure, which is shown in Figure 1.

Table 1 shows the considered loading states and corresponding criteria. The three states considered here are the serviceability limit, damage limit, and ultimate limit. The sectional force on the boundary part between the pile and spread foundation parts should be carefully considered. Thus, the analysis result was used to evaluate the sectional force on the boundary part. Note that, the torsion behavior of the foundation is also considered in the case of seismic load.

3. BUILDING A

3.1 Design Overview

Building A is a practical example, in which the design procedure is applied. Figure 2 shows the exterior of building A, which is surrounded by a dashed line, and is structurally separated from the other buildings by expansion joints. Figure 3 shows the foundation plan, and Figure 4 presents the cross-section. Building A is a high-rise building constructed with a steel structure, which is 88 m high and possesses 21 stories and two underground floor buildings. The construction area is approximately 91 m × 78 m. Underground floors were constructed in the area from line Y8 to Y13. The area from line Y5 to Y8 is partially included. These areas are supported by a spread

Table 1 Loading states and criteria

	Stationary load	Seismic load	
	Serviceability limit	**Damage limit**	**Ultimate limit**
Spread foundation bearing capacity	Maximum bearing pressure < Allowable pressure for sustained load	Maximum bearing pressure < Allowable pressure for temporary load	Maximum bearing pressure < Ultimate pressure capacity
Pile foundation bearing capacity	Load < Allowable load for sustained load	Load < Allowable load for temporary load	Load < Ultimate load
Stress on boundary section	Allowable stress for sustained load	Allowable stress for temporary load	Ultimate stress capacity

foundation. The bearing pressures of the foundations are 170–320 kN/m^2 (Figure 3). No underground floors are present in the other areas, located from line Y1 to Y7. These areas are supported by a pile foundation. The piles are bottom-enlarged piles with a 1.8 m diameter shaft and a 2.0 to 2.4 m diameter tip.

Figure 2 Exterior (building A)

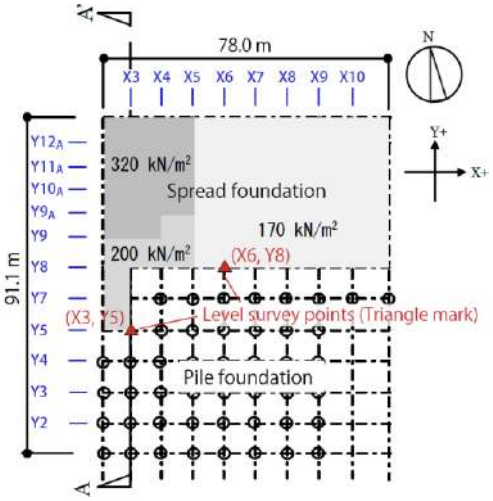

Figure 3 Foundation plan (building A)

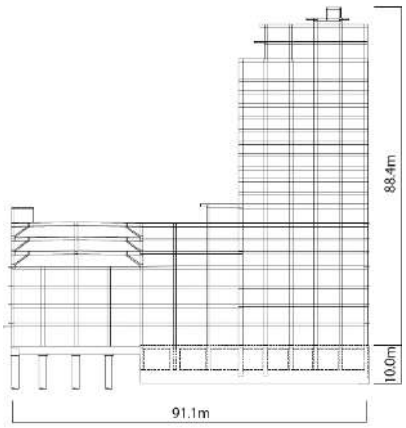

Figure 4 A-A' cross section (building A)

Figure 5 shows the geological cross-sections and *N*-values determined via a standard penetration test. The alluvium layers, composed of medium sand-gravel layers (Asg1 and Asg2) and a silty-clay layer (Asc), extend from the surface to a depth of ground level (G.L.) −7 m. Diluvium layers are located below them. Dense sand-gravel layers (Dg) extend from G.L. −7 m to approximately G.L. −10 m, above tuffaceous sands (Ot1 and Ot2) with an *N*-values of 50 or more, which are found from approximately G.L. −10 m to the bottom of investigated depth.

This Ot1 layer is a supporting layer. Both spread and pile foundations are embedded upon it.

The underground water level is at G.L. −1.6 m. Note that the strengths of the Asg1 and Asg2 against soil liquefaction were also checked (Architectural Institute of Japan, 2001), with the results indicating that they are sufficiently strong against soil liquefaction. Thus, we did not consider the soil liquefaction case.

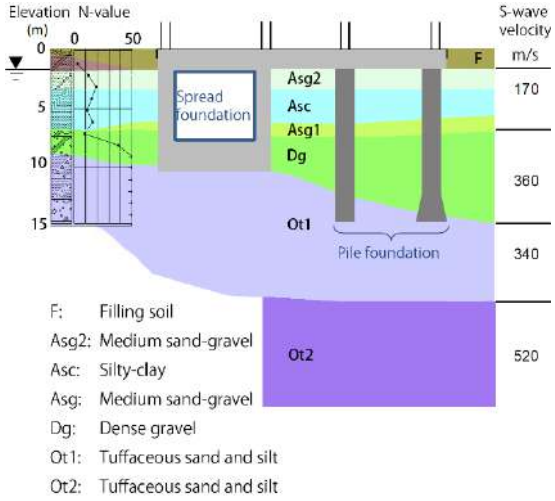

Figure 5 Geological cross section (buiding A)

3.2 Numerical Analysis

Based on the workflow in Figure 1, a static FEM deformation analysis was conducted after the cross-section of each component was provisionally decided from the frame model analysis. We used the commercial FEM analysis software, Soil Plus, for the static FEM analysis (Soil Plus, 2001). Figure 6 shows the FEM mesh. The ground, first-floor slab, and subsurface structure were modeled. The ground was 480 m in diameter and 130 m in depth from the building. Elasto-plastic solid elements were used for the soil elements. Table 2 shows the material constants of the soils. The initial Young's modulus of each soil E_{ps} was given as the Young's modulus under the micro-strain, which was based on the PS suspension logging results (Imai, 1977). For the nonlinear characteristics of the soil elements, the specific shear stiffness–shear strain relations shown in Figure 7 (Architectural Institute of Japan, 2001; Imazu and Fukutake, 2000) were used. The foundation structures and load conditions were established as discussed in the following section for the vertical and lateral load cases.

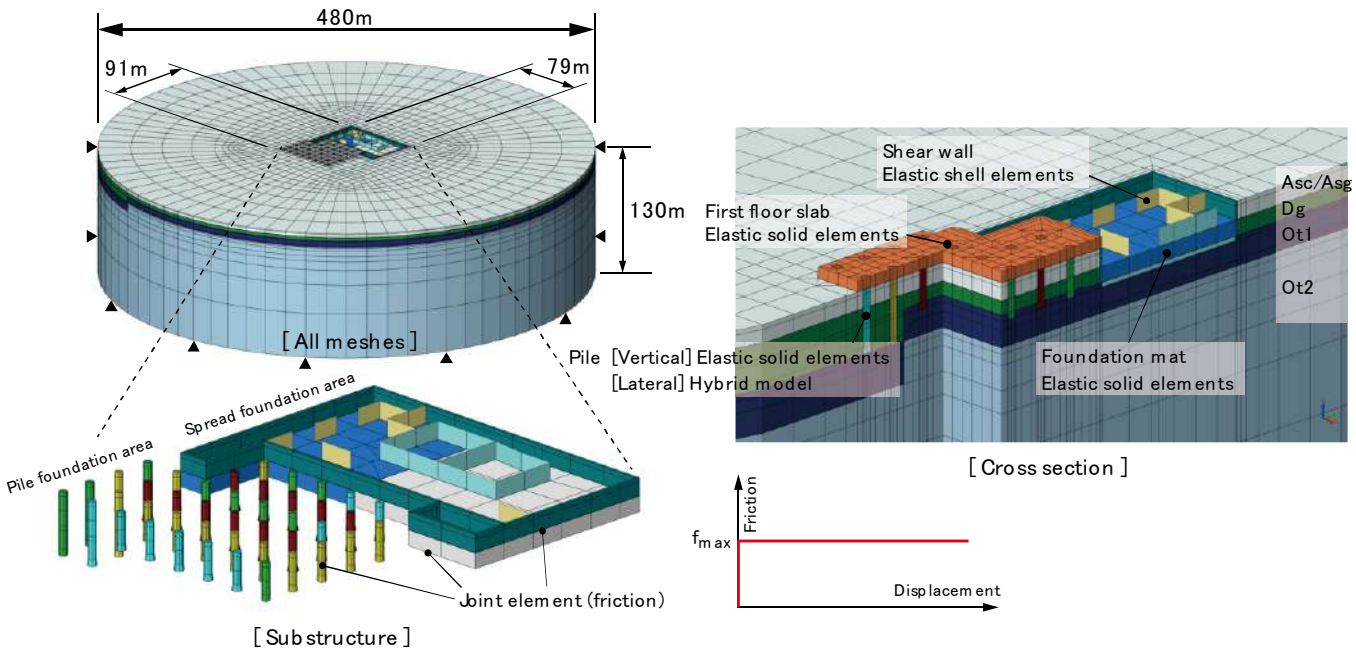

Figure 6 FEM mesh (building A)

Table 2 Material constant (building. A)

Name	V_s (m/s)	E_{ps} (kN/m^2)	ν	type	N-value	f_{max} (kN/m^2)
Asc/Asg	170	150,000	0.3	Sand	10	33
Dg	360	750,000	0.3	Gravel	50	100
Ot1	340	660,000	0.3	Sand	-	-
Ot2	520	1,370,000	0.3	Sand	-	-

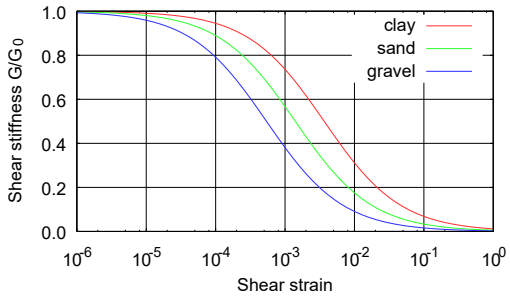

Figure 7 Shear strain-shear stiffnes relation

3.2.1 Vertical Load Analysis

Elastic solid elements were used for the floor slabs, underground outer walls, foundation mat, and piles. Elastic shell elements were used for the shear walls. Rigid-plastic joint elements were used for the interfaces between the soil and the pile shafts or underground outer walls to model contact-exfoliation and friction between the soil and the structure.

The spread foundation part was loaded by the concentrated loads at each column position, whereas the pile foundation part was loaded by the spread loads for each pile head.

Figure 8 and 9 shows the calculated vertical displacement and the calculated vertical axial stress of the soil, respectively. The analytical results indicate that the displacement around the spread and pile foundation parts were approximately 11 mm and 8 mm, respectively. The estimated differential settlements were not very strong and were, therefore, acceptable.

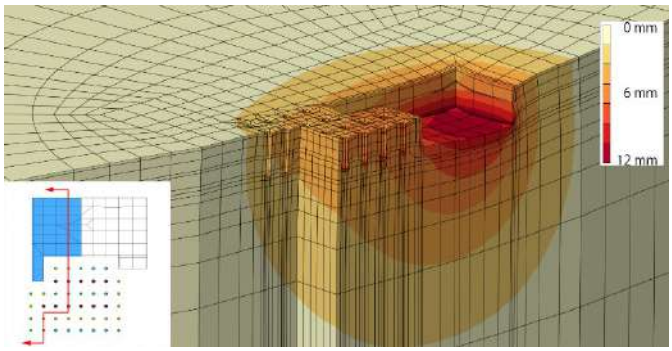

Figure 8 Computed vertical displacements (building A)

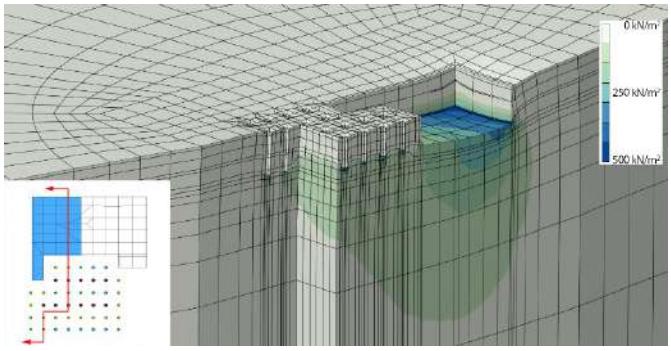

Figure 9 Computed vertical axial stress increments (building A)

3.2.2 Lateral Load Analysis

Elastic solid elements were used for the underground outer walls. The floor slabs and foundation mat were regarded as rigid plates. Elastic solid elements provided with sufficient Young's moduli were used for slabs and the foundation mat. Elastic shell elements were used for shear walls. The piles were modeled using a hybrid model composed of beam, solid, and shell elements (Figure 10). The beam

elements represented the bending and shear stiffness of the piles. The solid elements represented the pile volume, and were completely stiffness free. The plates were rigid, and were modeled using the pile model according to the Euler–Bernoulli beam assumption.

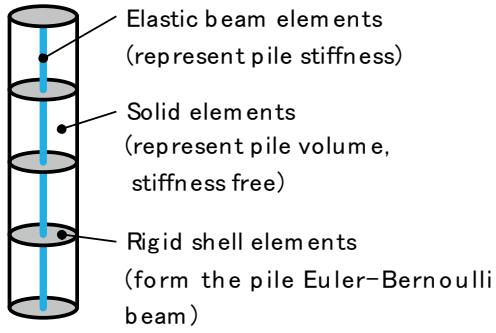

Figure 10 Hybrid pile model

Similar to the vertical load case, joint elements that represented the friction and contact-exfoliation behavior were used for the following interfaces: the soil and pile shafts, soil and underground outer walls, and the soil and foundation mat. The ultimate friction between the soil and foundation mat was set to 0.5 times that of the effective ground pressure.

The lateral loads were given at the center of gravity to the slab as a concentrated load. Four lateral load direction cases, namely, X+, X−, Y+ and Y−, were examined.

When designing the pile cross-sections, the ground displacements were also considered, in addition to the inertial force of the building calculated using the preceding FEM analysis. A response NULL displacement method was used to evaluate the sectional force of each pile. The ground displacements were calculated using an earthquake simulation program (Kurimoto et al., 2000) from the input earthquake wave on the engineering bedrock. These displacements were passed into a pile beam and soil spring model (Figure 11) as forced ground displacements. For the nonlinear characteristics of the subgrade reaction modulus, the tri-linear spring shown in Figure 12 was used in the response displacement analysis. This is a tri-linearized version of the square root relations of the displacement and subgrade reaction modulus shown in the Recommendations for Design of Building Foundations (RDBF) (Architectural institute of Japan, 2001).

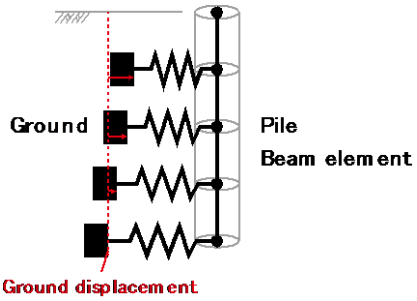

Figure 11 Pile beam and soil spring model

The final sectional force of the pile was calculated using the square root of the sum of the square of the sectional force from the inertial force and that from the ground displacement.

Figure 13 shows the calculated horizontal displacement under the loading in the X+ direction. Figure 14 presents the calculated axial stress in the X+ direction of the soil under the same loading condition. This behavior almost seems to translate to the X+ direction. The torsion behavior in the structural designing was negligibly small. The relatively large stress apparent in the ground in Figure 14 propagates from the spread foundation. The boundary between Ot1 and Ot2, which have different Young's moduli, causes the discontinuity in the stress distribution.

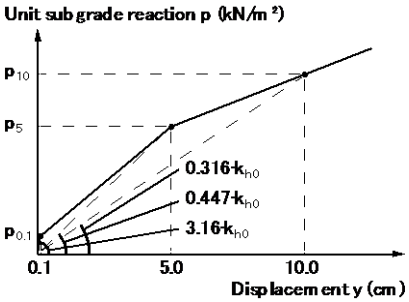

* k_{h0}: Subgrade reaction modulus for lateral load under unit pile head displacement (1 cm).

Figure 12 Tri-linear spring

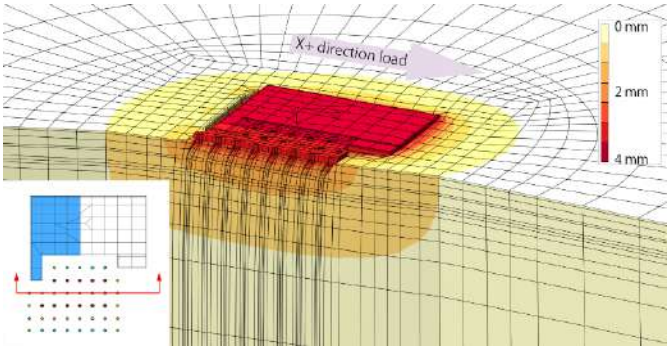

Figure 13 Computed displacements in X+ direction (building A)

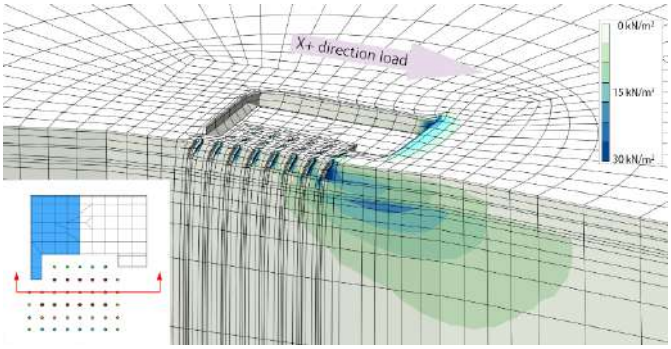

Figure 14 Computed holizontal axial stress increments (building A)

Table 3 shows the load-sharing ratio at each part of the foundation under loading in the X+ and Y+ directions. The ratio of the spread and pile foundation parts was approximately 8:2. The ratio of the bottom face of the spread foundation was noticeably high, and shared approximately half the total load. The ratio of the underground outer wall, passive pressure, and skin friction was essentially in accordance with the area ratio.

The load-sharing ratio of the pile foundation part was notably small, because of the spread foundation carrying the bulk of the lateral load. We confirmed that the sectional forces for each pile were smaller than the allowable stress for the temporary or ultimate load.

Table 3 Load sharing ratio (building. A) (unit: %)

		Direction			
		X+		Y+	
Total load		100		100	
Load shared by spread foundation	Bottom friction	79	53	77	49
	Wall pressure		13		17
	Wall friction		13		11
Load shared by pile		21		23	

3.3 Measurements

We measured the actual settlements of the building on the site, using an optical level. The reference points were placed on the existing structure supported by the bearing pile. They measured at two time points. The first measurements were taken only after the first floor was placed. The second measurements were taken upon construction completion. In the discussion that follows, each settlement value is the difference between these two measurements.

The measurements were taken at the (X6, Y8) and (X3, Y5) points shown in Figure 3. Table 4 presents the measured settlements at 8 and 4 mm. The resolution of these measurements was small compared with that of the optical level measurements. A variance of ±3 mm may also be noted in the measurements. Compared with the FEM prediction, the measured settlements were similar to those of the FEM at point (X6, Y8) or slightly smaller than those at point (X3, Y5).

Table 4 Measured settlement (building. A)

	(X6, Y8)	(X3, Y5)
Calculated	8 mm	7 mm
Measured	8 mm	4 mm

The FEM prediction also showed slightly greater settlement than the actual settlement. This difference may have been caused by the use of certain parameter (e.g., maximum friction) values different to the actual values, for improved robustness against property variance. This practice is often referred to as taking parameters “on the safe side”. This issue is also discussed in section 4.4 below.

4. BUILDING B

4.1 Design Overview

Building B is the second example considered in this paper. Figure 15 shows the exterior of building B and Figure 16 presents the foundation plan. Figure 17 illustrates the cross-section. The building was constructed with steel and reinforced concrete. Some parts were constructed with concrete encased steel column. This building is 70 m high and possesses 14 stories. The construction area is about 46 m × 44 m with a base isolation layer below the first floor slab. Underground floors were built in the area from lines 1 to 3. These areas are supported by a spread foundation. The foundation bearing pressure is 330 kN/m^2 (Figure 16). No underground floors were built in the other area, from lines 3 to 6. These areas are supported by a pile foundation. Figure 18 shows the geological cross-sections and *N*-values investigated via a standard penetration test. The filling soil (Bs) and loose silty-sand layer (Asc) extend from the surface to a depth of G.L. −16m. Diluvium layers exist below them. Dense sand/gravel layers (Dsx/ Dgx) alternate with high-plasticity clay layers (Dcx). All piles, except C4 and C5, are supported by a Ds1 layer (G.L. −16 m). The C4 and C5 piles are supported by a Dg1 layer (G.L. −35 m).

Figure 15 Exterior (building B)

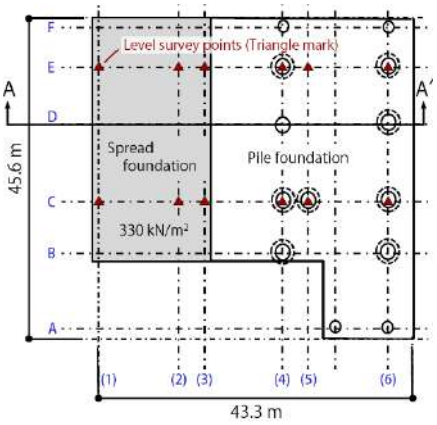

Figure 16 Foundation plan (building. B)

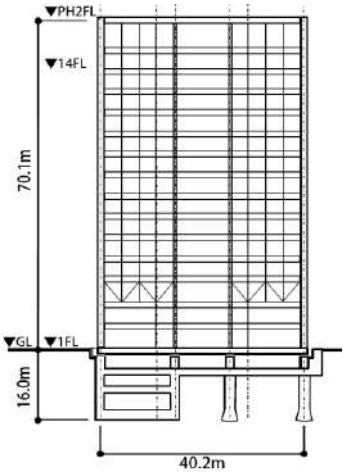

Figure 17 A-A' cross section (building. B)

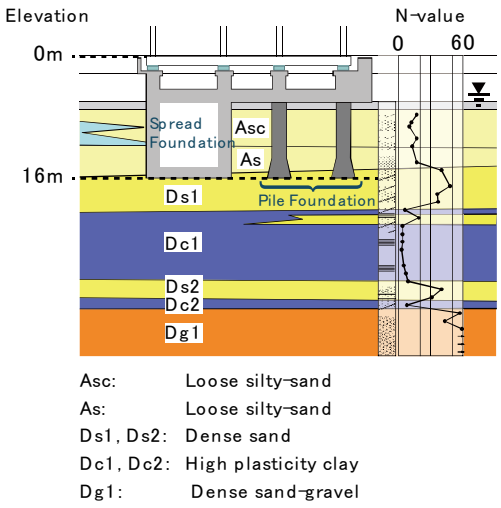

Figure 18 Geological cross section (building. B)

The underground water level is at G.L. −2.4 m. The strength of the Bs and Asc against soil liquefaction were also checked. The fine fraction content of the Asc is approximately 10 - 17%. The liquefaction evaluation results show that the Asc may not liquefy in the damage limit state (approximately 200 cm/s^2 ground acceleration), but may liquefy in the ultimate limit state (approximately 350 cm/s^2 ground acceleration). Therefore, we also consider the case in which this layer is liquefied.

4.2 Numerical Analysis

The building B foundation was evaluated, similar to building A. The FEM modeling concept was almost the same as that used for building A. Figure 19 shows the FEM mesh. The ground, first-floor slab, and sub-surface structure were modeled. The ground was to have a 200 m diameter and 65 m depth from the building. Elasto-plastic solid elements were used for soil elements.

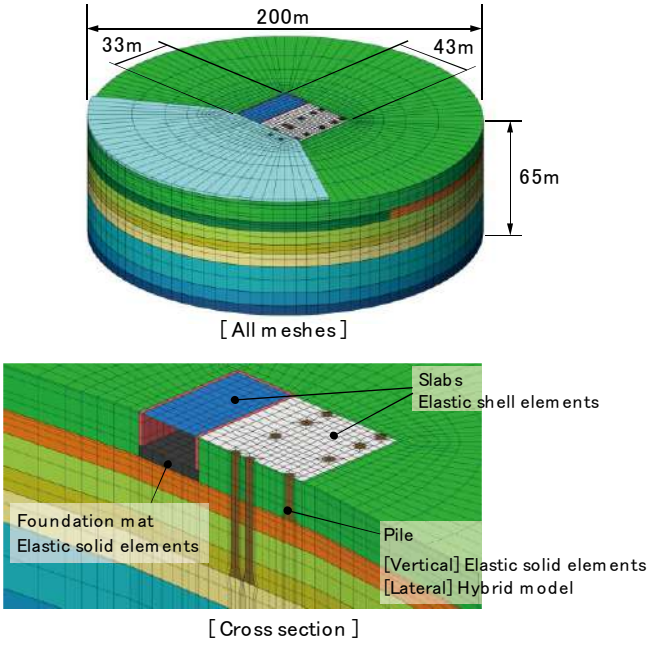

Figure 19 FEM model (building B)

Table 5 (a) shows the material constants of the soils. The Ds1 layer, which is a supporting layer for both the pile and spread foundations, had an *N*-value variance according to the planar position. Therefore, two Ds1 layers were considered: Ds1a from lines A to C, with an *N*-value of 40, and Ds1b from lines C to F with an *N*-value of 60. The material constants used for liquefied soil are also listed in Table 5 (b). We followed the stiffness reduction factor given in the RBDF (Architectural Institute of Japan, 2001). Under the assumption that the sand stiffness is proportional to the square root of its effective stress, the RBDF gives an estimate of the stiffness reduction factor of liquefied sand as being 0.02 - 0.08 when the conversion *N*-value, incorporating the effect of the fine fraction content, is

Table 5 (a) Material constant (building B)

Name	Bottom (G.L. −m)	E_{ps} (kN/m^2)	v	type	*N*-value	f_{max} (kN/m^2)
Bs	4	120,000	0.30	Sand	5	17
Asc	15	220,000	0.30	Sand	12	40
Ds1a	20	520,000	0.30	Sand	60	100
Ds1b		400,000		Sand	40	
Dc1	27	190,000	0.45	Clay		100
Ds2/Dc2	32	340,000	0.30	Sand	20	66
Dg1	39	760,000	0.30	Sand-gravel	-	-
Dc3	53	260,000	0.45	Clay	-	-
Ds3	60	850,000	0.30	Sand	-	-
Dg2	62	1,700,000	0.30	Sand-gravel	-	-

Table 5 (b) Material constant (liquefied version) (building B)

Name	Bottom (G.L. −m)	E_{ps} (kN/m^2)	v	type	*N*-value	f_{max} (kN/m^2)
Bs	4	6,000	0.30	Sand		
Asc	15	11,000	0.30	Sand		

V_s: Shear wave velocity
E_{ps}: Initial Young's modulus of soil investigated via PS suspension logging
v: Poisson ratio
f_{max}: Maximum friction between pile and soil

20 – 30. Further, the RBDF estimates that the subgrade reaction modulus is reduced by 0.05 – 0.20 times its normal value. We followed these estimates and set the liquefied versions of the E_{ps} values of the layers to 0.05 times of initial E_{ps}. The foundation structures and load conditions for the vertical and lateral load cases are established in the discussion that follows.

4.2.1 Vertical Load Analysis

Elastic solid elements were used for the underground outer walls, foundation mat, and piles. Meanwhile, elastic shell elements were used for the floor slabs. Rigid-plastic joint elements were used for the interfaces between the soil and the pile shafts or underground walls.

The load conditions were almost the same as those in building A. Concentrated loads were used for the spread foundation part, whereas spread loads were used for the pile foundation part.

We first attempted to embed all piles in the Ds1 layer at the same pile length. However, a large displacement around the C4 and C5 piles was found in the first FEM analysis. We refined the pile length of these two piles so that they were supported by the Dg1 layer at G.L. −35 m, and looped back to the FEM analysis stage.

Figure 20 shows the calculated vertical displacement of the definitive design. Figure 21 also presents the calculated vertical axial stress of the soil. The analysis results indicate that the displacement around the spread foundation part was approximately 22 mm. Meanwhile, the displacement around the pile foundation part was almost identical to that of the spread foundation, at 20 mm. The compression of the C4 and C5 piles was approximately 8 mm. The estimated differential settlements were acceptable.

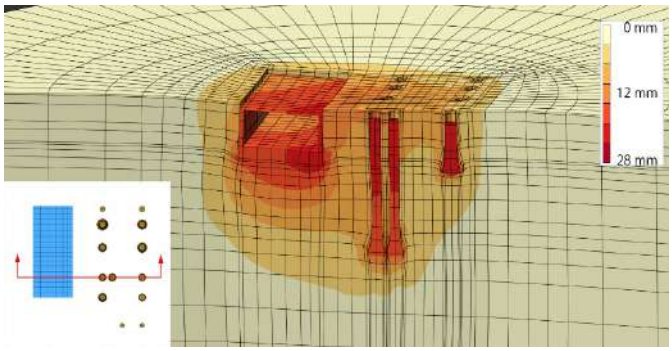

Figure 20 Computed vertical displacement (building B)

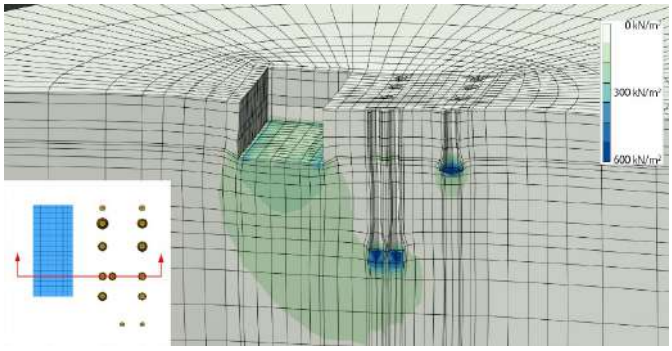

Figure 21 Computed vertical axial strss increments (building B)

4.2.2 Lateral Load Analysis

For the underground outer walls, elastic shell elements were used. The floor slabs and foundation mat were regarded as rigid plate. The piles were modeled by hybrid model shown in Figure 10.

The joint elements for the interfaces between the soil and pile shafts, underground walls or foundation mat were the same as those in building A. The lateral loads were given at the center of gravity of the slab as concentrated loads. Eight analysis cases were considered from four lateral load direction cases, namely, X+, X−, Y+ and Y−. In addition, two As layer condition cases were included, in which the layer was or was not liquefied.

The ground displacements calculated via the response displacement method were also considered to determine the pile cross-section design.

Figure 22 shows the calculated horizontal displacement under the loading in the X− direction when the As layer was liquefied. Figure 23 presents the calculated horizontal axial stress under the same conditions. This behavior almost seemed to translate in the X− direction. The stress was distributed in a small area near the underground walls or piles.

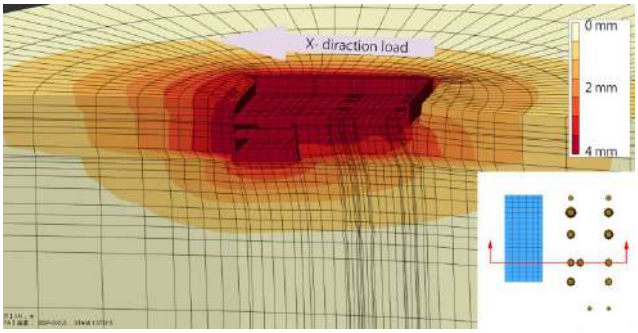

Figure 22 Computed displacements in X− direction (building B)

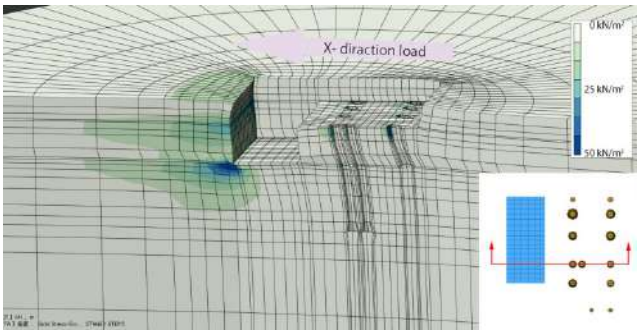

Figure 23 Computed horizontal axial stress increments (building B)

Table 6 shows the load-shearing ratio at each part of the foundation in each case. The ratio of the spread foundation part and pile foundation part was approximately 8:2. The ratio of the bottom face of the spread foundation was still high, and shared about 29–46% of the total load. The load-sharing ratio of the bottom face of the spread foundation increased slightly when the As layer was liquefied. Moreover, low correspondence between the load-shearing ratio and load direction was observed.

We confirmed that the sectional forces of the pile were smaller than the allowable stress for the temporary or ultimate load. We also confirmed that the safety factor is greater than 2 for each pile.

The FEM analysis result showed no torsion behavior. The fact that building B was designed to have the center of gravity and the center of rigidity close together contributed greatly to the reduction of torsion. The sufficiently embedded underground part caused by the base isolation layer also contributed to the reduction of the foundation torsion behavior.

Table 6 Load sharing ratio (building B) (unit: %)

			Direction							
			X+		X−		Y+		Y−	
No liquefaction (damage limit)	Total load		100		100		100		100	
	Load shared by spread foundation	Bottom friction		33		27		32		29
		Wall pressure	81	22	76	26	78	21	78	23
		Wall friction		26		23		25		26
	Load shared by pile foundation		19		24		22		22	
Liquefied alluvium (ultimate limit)	Total load		100		100		100		100	
	Load shared by spread foundation	Bottom friction		46		41		43		42
		Wall pressure	84	16	78	19	79	20	79	17
		Wall friction		22		18		16		20
	Load shared by pile foundation		16		22		21		21	

4.3 Measurements

The actual settlement of the base isolation layer in building B was measured.

The measurements were taken at the point marked by triangles in Figure 16, using an optical level in the same manner as for the building A case. Figure 24 shows the settlements on lines C and E, which were 15 - 20 mm on average. The settlements on line C were slightly smaller than those of line E. Compared with the FEM prediction, the absolute value of the settlement calculated by the FEM analysis was slightly larger than the actual settlement, especially on line C. However, the differential settlement prediction provided by the FEM analysis corresponded well with the actual differential settlements. The maximum slab gradient caused by the differential settlement was 0.56×10^{-3}. The gradient was within the acceptable range of 1.00×10^{-3}.

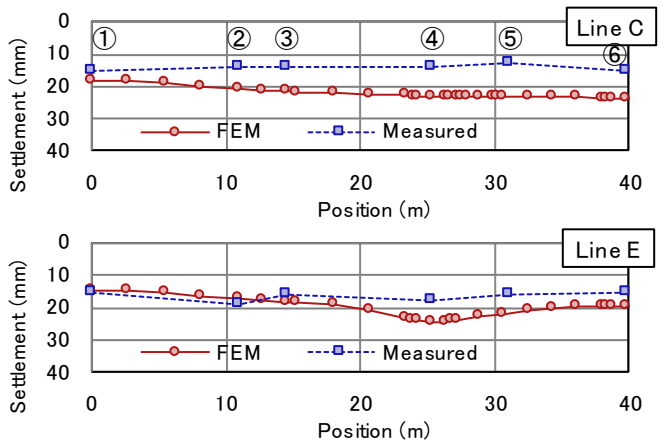

Figure 24 Measured settlement (building B)

4.4 Discussion

The differential settlement distribution of the FEM prediction is sufficiently similar to the actual distribution. However, the settlement given by the FEM prediction is slightly greater than the actual settlement, especially in the pile foundation part.

This difference exists because of the following reasons. In the structural design, it is assumed that the superstructure is completely supported by the pile foundation. In other words, the structural design ignores the bearing pressure of the slab in the pile foundation part. Our FEM model follows the assumption that the floor slab element is not in contact with the ground surface. However, the floor slab laid on the ground surface is in contacts with the ground. Moreover, the bearing pressure of the slab may affect the settlement behavior.

Figure 25 shows another FEM result, which is the case where the slab nodes are connected with the ground nodes. The calculated settlement of the pile foundation is reduced significantly. As a whole, this result corresponds well with the measured data.

Contrary to the FEM result used in the design procedure, the result shown in Figure 25 provides slightly lesser settlement, which may be because the pile foundation is not a piled-raft foundation. The bottom of the footing beams may be in good contact with the ground. They carry some of the load as their bearing pressure. Meanwhile, it is uncertain whether the floor slabs are in contact with the ground. They cannot be expected to form a complete foundation mat. Figure 25 shows that the slab carries 20% of the total load in building B.

This study implies that the pile foundation part takes some of the resistant force from the bearing pressure of the slab or footing beam. However, the force is smaller than that of the piled-raft foundation.

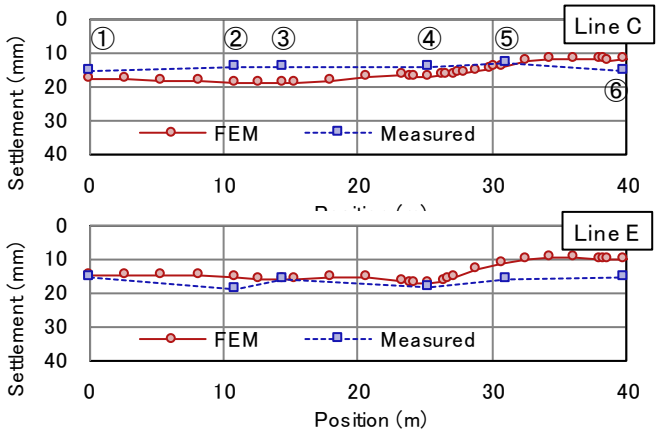

Figure 25 Measured and re-calculated settlement: Slab nodes are connected with the ground nodes (building B)

5. SUMMARY

This study introduced two practical examples of composite foundations. The concept, design procedure, and FEM analysis were also shown. We obtained an appropriate structural design for the vertical loads. This design did not cause a detrimental differential settlement using the presented procedure. We also measured the actual settlement for both examples. We found that the measured settlements were almost the same as or smaller than the estimated settlement. In addition, we obtained a more reasonable calculation result by considering the bearing pressure of the slab and the footing beam, similar to the piled-raft foundation. The study implies that the pile foundation part takes some of the resistant force from the bearing pressure of the slab or footing beam. Meanwhile, the bearing pressure of the pile foundation slab was smaller than that of the piled-raft full installation.

We confirmed that the sectional forces for the lateral loads were within the acceptable range. Moreover, the foundation did not cause detrimental torsion. The calculated torsion behavior was

significantly smaller than expected. The reasons are as follows: the spread foundation was large enough to carry the bulk of the lateral load. The underground walls of the embedded spread foundation helped in this regard. In addition, the building B was designed to have the center of gravity and the center of rigidity close together. Nevertheless, the torsion behavior was not a significant problem in these cases; this has been a topic of considerable interest in the composite foundation design. In addition to the bearing pressure of the slab and the footing beam in the vertical load case, the area ratio of the pile and spread foundation parts, embedded depth, and the eccentricity of the center of gravity will also provide future research directions.

6. REFERENCES

Architectural Institute of Japan. Recommendations for design of building foundations. Architectural Institute of Japan, 2001.

Coyle H. M. and Reese L. C. Load transfer for axially loaded piles in clay. ASCE, Vol. 92, No. SM2, 1–26, 1966.

Imai T. P and S wave velocities of the ground in Japan. Proc. 9th ICSMFE, Tokyo, Vol.2, 1977.

Imazu M. and Fukutake K. Dynamic shear modulus and damping of gravel materials. The 21th Japan National Conference on Soil Mechanics and Foundation Engineering, 509–512, Jun., 1986.

Kraft K. M., Ray R. P. and Kagawa T. Theoretical t-z curves. ACSE, Vol. 107, No. GT11, 1543–1561, 1981.

Kurimoto O., Fujimori T., Yasui Y. Seismic response of pile-supported structure considering nonlinearity of super-structure and pile and liquefaction of surrounding ground. Report of Obayashi Corp. Technical Research Institute, No. 60, 73–80, 2000.

Sahara M. Aseismic design for composite foundations. Annual meeting panel discussion report (Kanto), structural division, foundation structure, 79–84, 2015.

Soil Plus, Theory Manual of static. ITOCHU Techno-solutions Corp.